A Benchmark Case for Computational Acoustics including Rotating Domains

Manfred Kaltenbacher[1], Andreas Hüppe[1], Barbara Wohlmuth[2]
[1] TU Wien, Austria, Email {manfred.kaltenbacher,andreas.hueppe}@tuwien.ac.at
[2] TU München, Germany, Email Barbara Wohlmuth wohlmuth@ma.tum.de

Introduction

The numerical simulation of acoustic fields including rotating domains is still a great challenge and a topic of ongoing research. Therefore, it is our goal to setup a benchmark case, which will support research groups to develop their numerical solution approaches. We use a rotating point source, for which an analytical solution exists. Our approach is based on the Finite Element (FE) method, uses an Arbitrary Lagrangian Eulerian (ALE) framework and results in a convective wave equation for the scalar acoustic potential. Numerically, we explore the capability of nonconforming grids by applying a Nitsche-type mortaring between stationary and rotating regions. The formulation can be applied to classical acoustics (stagnant fluid) as well as moving fluids in the case of aeroacoustics.

We will make all results available to the European Acoustics Association (EAA) benchmark platform, which was initiated recently (see https://www.euracoustics.org/technical-committees/tc-on-computational-acoustics).

Analytic Solution of a Rotating Point Source

The generated sound field of a point source with strength $q(t)$, moving subsonically along the path $\boldsymbol{x} = \boldsymbol{x}_\mathrm{s}(t)$ is described by the following partial differential equation (PDE)

$$\frac{1}{c^2}\frac{\partial^2 \psi_\mathrm{a}}{\partial t^2} - \Delta\psi_\mathrm{a} = q(t)\,\delta(\boldsymbol{R}(t))\,; \quad \boldsymbol{R}(t) = \boldsymbol{x} - \boldsymbol{x}_\mathrm{s}(t)\,. \tag{1}$$

In (1) ψ_a denotes the scalar acoustic potential, c the speed of sound and $\boldsymbol{R}(t)$ the distance between source location $\boldsymbol{x}_\mathrm{s}$ and the observer location $\boldsymbol{x}$. This PDE can be analytically solved by the help of the free field Green's function (source coordinate $\boldsymbol{y}$, observer coordinate $\boldsymbol{x}$)

$$G(\boldsymbol{x},\boldsymbol{y},t,\tau) = \frac{\delta\left(t-\tau-\frac{|\boldsymbol{x}-\boldsymbol{y}|}{c}\right)}{4\pi|\boldsymbol{x}-\boldsymbol{y}|}\,, \tag{2}$$

and the acoustic potential ψ_a computes as

$$\psi_\mathrm{a}(\boldsymbol{x},t) = \frac{1}{4\pi}\int\limits_{-\infty}^{\infty}\frac{q(\tau)}{R(\tau)}\,\delta\left(t-\tau-\frac{R(\tau)}{c}\right)\mathrm{d}\tau \tag{3}$$

with $R = |\boldsymbol{R}|$. Using the delta function property

$$\begin{aligned}\int\limits_{-\infty}^{\infty}\delta\left(h(\tau)\right)\,g(\tau)\,\mathrm{d}\tau &= \sum_i \frac{g(\tau_i)}{|h'(\tau_i)|} \qquad (4)\\ h' &= \partial h/\partial\tau\,;\; h(\tau_i)=0\,,\end{aligned}$$

where the summation runs over all the zeros of h, this representation may be reduced to the Lienhard-Wiechert potential [1]

$$\begin{aligned}\psi_\mathrm{a}(\boldsymbol{x},t) &= \frac{q_\mathrm{e}(t)}{4\pi R_\mathrm{e}\left(1-M_\mathrm{e}\cos\vartheta_\mathrm{e}\right)} \qquad (5)\\ M_\mathrm{e} &= |\boldsymbol{M}_\mathrm{e}| = \left|\frac{1}{c}\,\frac{\partial\boldsymbol{x}_\mathrm{s}}{\partial t}\right|_{t_\mathrm{e}}\right|\,.\end{aligned}$$

Here, the subscript e denotes the evaluation at time t_e (retarded time or sometimes also called emission time), which computes by the nonlinear relation according to

$$c\,(t-t_\mathrm{e}) - R_\mathrm{e} = 0\,. \tag{6}$$

Furthermore, ϑ_e is the angle between source velocity $\partial\boldsymbol{x}_\mathrm{s}/\partial t_\mathrm{e}$ and distance vector $\boldsymbol{R}$ and computes by

$$\cos\vartheta_\mathrm{e} = \frac{\boldsymbol{R}_\mathrm{e}\cdot\boldsymbol{M}_\mathrm{e}}{R_\mathrm{e}M_\mathrm{e}}\,. \tag{7}$$

In order to arrive at the acoustic pressure, we have to compute the derivative with respect to time t and scale the result by the mean density ρ_0

$$p_\mathrm{a} = \rho_0\frac{\partial\psi_\mathrm{a}}{\partial t}\,. \tag{8}$$

Since (5) is a function of t_e, we use (6) to obtain

$$\begin{aligned}\frac{\partial t}{\partial t_\mathrm{e}} &= \frac{1}{c}\frac{\partial R_\mathrm{e}}{\partial t_\mathrm{e}} + 1 = \frac{1}{c}\frac{\partial|\boldsymbol{x}-\boldsymbol{x}_\mathrm{s}|}{\partial t_\mathrm{e}} + 1\\ &= 1 - \frac{\boldsymbol{R}_\mathrm{e}\cdot\boldsymbol{M}_\mathrm{e}}{R_\mathrm{e}} = 1 - M_\mathrm{e}\cos\vartheta_\mathrm{e}\,. \qquad (9)\end{aligned}$$

Substituting (5) into (8) we obtain for the acoustic pressure the following relation

$$\begin{aligned}p_\mathrm{a} &= \frac{\rho_0\frac{\partial q_\mathrm{e}}{\partial t}\,R_\mathrm{e}\left(1-M_\mathrm{e}\cos\vartheta_\mathrm{e}\right)}{4\pi R_\mathrm{e}^2\left(1-M_\mathrm{e}\cos\vartheta_\mathrm{e}\right)^2}\\ &\quad - \frac{\rho_0 q_\mathrm{e}\frac{\partial}{\partial t}\left(R_\mathrm{e}\left(1-M_\mathrm{e}\cos\vartheta_\mathrm{e}\right)\right)}{4\pi R_\mathrm{e}^2\left(1-M_\mathrm{e}\cos\vartheta_\mathrm{e}\right)^2}\,. \qquad (10)\end{aligned}$$

Using (6) and (9) we may write

$$\frac{\partial R_\mathrm{e}}{\partial t} = c\left(1-\frac{\partial t_\mathrm{e}}{\partial t}\right) = -c\frac{M_\mathrm{e}\cos\vartheta_\mathrm{e}}{1-M_\mathrm{e}\cos\vartheta_\mathrm{e}}\,. \tag{11}$$

Now, we explore (7) and use (9) to obtain

$$\begin{aligned}\frac{\partial}{\partial t}\left(R_\mathrm{e}M_\mathrm{e}\cos\vartheta_\mathrm{e}\right) &= \frac{\partial}{\partial t_\mathrm{e}}\left(\boldsymbol{R}_\mathrm{e}\cdot\boldsymbol{M}_\mathrm{e}\right)\,\frac{\partial t_\mathrm{e}}{\partial t}\\ &= \frac{\boldsymbol{R}_\mathrm{e}\cdot\boldsymbol{M}_\mathrm{e}' + \boldsymbol{R}_\mathrm{e}'\cdot\boldsymbol{M}_\mathrm{e}}{1-M_\mathrm{e}\cos\vartheta_\mathrm{e}}\,. \qquad (12)\end{aligned}$$

Thereby, we use the symbol $'$ to denote the derivative with respect to t_e, and the term $\boldsymbol{R}'_\mathrm{e}$ calculates as

$$\boldsymbol{R}'_\mathrm{e} = \frac{\partial}{\partial t}\left(\boldsymbol{x} - \boldsymbol{x}_\mathrm{s}(t_\mathrm{e})\right) = -c\boldsymbol{M}_\mathrm{e}\,. \tag{13}$$

Collecting all these results, we may compute the acoustic pressure by

$$p_\mathrm{a} = \rho_0 \frac{q'_\mathrm{e}}{4\pi R_\mathrm{e}\left(1 - M_\mathrm{e}\cos\vartheta_\mathrm{e}\right)^2} + \rho_0 q_\mathrm{e} \frac{\boldsymbol{R}_\mathrm{e}\cdot\boldsymbol{M}'_\mathrm{e} + cM_\mathrm{e}\left(\cos\vartheta_\mathrm{e} - M_\mathrm{e}\right)}{R_\mathrm{e}^2\left(1 - M_\mathrm{e}\cos\vartheta_\mathrm{e}\right)^3}\,. \tag{14}$$

Formulation

We have to start at the basic equations for fluid dynamics, which are defined for an Eulerian framework. Since in our case we have stationary and rotating domains, an Arbitrary Lagrangian Eulerian (ALE) description is necessary. Therefore, the conservation of mass and momentum read as [2]

$$\frac{\partial\rho}{\partial t} + \boldsymbol{v}_\mathrm{c}\cdot\nabla\rho = -\rho\nabla\cdot\boldsymbol{v} \tag{15}$$

$$\rho\frac{\partial\boldsymbol{v}}{\partial t} + \left(\rho\boldsymbol{v}_\mathrm{c}\cdot\nabla\boldsymbol{v} = -\nabla p + \nabla\cdot\boldsymbol{\tau}\,. \right. \tag{16}$$

Thereby, ρ denotes the fluid density, $\boldsymbol{v}$ the fluid velocity, $\boldsymbol{v}_\mathrm{c}$ the convective velocity, p the fluid pressure and $\boldsymbol{\tau}$ the viscous stress tensor. For stagionary domains $\boldsymbol{v}_\mathrm{c}$ is simply the fluid velocity $\boldsymbol{v}$, and for rotating domains it computes by $\boldsymbol{v} - \boldsymbol{v}_\mathrm{r}$ with $\boldsymbol{v}_\mathrm{r}$ being the velocity at each point of the rotating domains.

Now, we assume an isentropic case, where the total variation of the entropy is zero and the pressure is only a function of the density. Furthermore, we neglect the viscous stress tensor and perform a perturbatuion ansatz

$$p = p_0 + p_\mathrm{a}\,;\ \rho = \rho_0 + \rho_\mathrm{a}\,;\ \boldsymbol{v} = \boldsymbol{v}_\mathrm{a}\,, \tag{17}$$

with $p_\mathrm{a} \ll p_0$ and $\rho_\mathrm{a} \ll \rho_0$. In addition, we assume a spatial and temporal constant mean density ρ_0 and pressure p_0. Substituting (17) into (15) and (16) results after linearisation in the conservation equations for linear acoustics

$$\frac{\partial\rho_\mathrm{a}}{\partial t} - \boldsymbol{v}_\mathrm{r}\cdot\nabla\rho_\mathrm{a} + \rho_0\nabla\cdot\boldsymbol{v}_\mathrm{a} = 0 \tag{18}$$

$$\rho_0\frac{\partial\boldsymbol{v}_\mathrm{a}}{\partial t} - \rho_0\boldsymbol{v}_\mathrm{r}\cdot\nabla\boldsymbol{v}_\mathrm{a} + \nabla p_\mathrm{a} = 0\,. \tag{19}$$

Using the scalar acoustic potential ψ_a, we may rewrite (19) by

$$\nabla_{p_\mathrm{a},\psi_\mathrm{a}}\left(\rho_0\frac{\partial\psi_\mathrm{a}}{\partial t} + \rho_0\boldsymbol{v}_\mathrm{r}\cdot\nabla\psi_\mathrm{a} + p_\mathrm{a}\right) = 0\,. \tag{20}$$

In (20) the nabla operator $\nabla_{p_\mathrm{a},\psi_\mathrm{a}}$ means that it just operates on p_a and ψ_a. Furthermore, we have used the equivalence of

$$\rho_0\boldsymbol{v}_\mathrm{r}\cdot\nabla\left(\nabla\psi_\mathrm{a}\right) = \nabla_{\psi_\mathrm{a}}\left(\rho_0\boldsymbol{v}_\mathrm{r}\cdot\nabla\right)\psi_\mathrm{a}\,.$$

From (20), we obtain the expression for the acoustic pressure by

$$p_\mathrm{a} = \rho_0\frac{\partial\psi_\mathrm{a}}{\partial t} - \rho_0\boldsymbol{v}_\mathrm{r}\cdot\nabla\psi_\mathrm{a} = \rho_0\frac{D\psi_\mathrm{a}}{Dt}\,;\ \frac{D}{Dt} = \frac{\partial}{\partial t} - \boldsymbol{v}_\mathrm{r}\cdot\nabla\,. \tag{21}$$

Finally, we substitute (21) into (18) and arrive at

$$\frac{1}{c^2}\frac{D^2\psi_\mathrm{a}}{Dt^2} - \Delta\psi_\mathrm{a} = 0\,. \tag{22}$$

For the numerical solution of (22) we apply the Finite-Element (FE) method. Thereby, we explore the capability of nonconforming grids by applying a Nitsche-type mortaring between stationary and rotating regions (for details see [3, 4]).

As already stated for stationary nonconforming meshes, spurious waves, which are not resolved by the discretization (both in space and time), deteriorate the numerical solution and should be numerically damped. Since numerical damping cannot be introduced in the classical Newmark method without degrading the order of acccuracy [5], we advise to apply a time-stepping scheme with controlled numerical dispersion such as the HHT (Hilber-Hughes-Taylor) method [5]. Thereby, three parameters define the behavior of the time-stepping scheme: α_HHT, β_HHT and γ_HHT. The HHT method is unconditional stable and 2^nd order accurate for $\alpha_\mathrm{HHT} \in [-0.3, 0)$ and according to the choice of this parameter introduces numerical damping. The two other parametrs compute as

$$\beta_\mathrm{HHT} = \frac{(1-\alpha_\mathrm{HHT})^2}{4}\,;\quad \gamma_\mathrm{HHT} = \frac{(1-2\alpha_\mathrm{HHT})}{2}\,.$$

For a detailed analysis, we refer to [5].

Computational Setup and Results

The computational setup is displayed in Fig. 1. We consider in the inner domain a small disc with radius $R = 0.2123\,\mathrm{m}$ rotating at 2000 rpm, on which a point source with initial coordinates $(0.1, 0, 0)^t$ is located and emits sound at a frequency f_s of 500 Hz. The surrounding stationary subdomain is a block with side length $1.8\,\lambda$

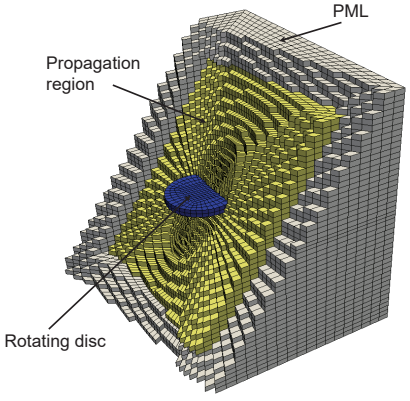

Figure 1: Rotating disc inside a stationary propagation region surrounded by a perfectly matched layer (PML).

($\lambda = c/f = 0.68\,\mathrm{m}$) being enclosed by a PML-region of thickness $\lambda/4$. The fixed observation point is at position $(0.9\lambda, 0, 0)^t\,\mathrm{m} = (0.6123, 0, 0)^t\,\mathrm{m}$. The number of FE nodes and elements are listed in Tab. 1. The mesh consists of pure hexhaedral elements using first order (bilinear) basis functions.

	Nodes	Elements
Rotating disc	432	492
Propagation	77.318	143.664
PML	94.964	162.552

Table 1: FE nodes and elements in the different regions.

The space discretization is chosen by $h \approx \lambda/17$ and the time step size is set to $\Delta t = 1/(80 f_\mathrm{s}) = 25\,\mu\mathrm{m}$. As time discretization we apply the HHT-scheme with parameters as discussed in the previous section.

Although this example seems to be very simple, it has for any domain discretization approach the following challenges:

1. The rotating and the stationary domains have to be discretized and need an appropriate numerical scheme for the coupling at the interface. We use a Nitsche-type mortaring, see [3].
2. Since the setup with the rotating point source belongs to the class of free radiation, the numerical scheme needs an appropriate method at the boundary of the computational domain. We apply an advanced PML-method in time domain as presented in [6].
3. It is a time domain problem and although we do not include scatterer in the rotating as well as stationary domain, it includes the challenges as one can find in real axial and/or radial fans.

In a first step, we compute the acoustic scalar potential ψ_a and compare it to the analytic solution for one revolution of the point source after achieving steady state (see Fig. 2). In order to reduce transient oscillation, we use a smooth fade-in function, so that our point excitation $q(t)$ computes by

$$q(t) = \begin{cases} \sin(2\pi f_\mathrm{s} t)\,(1 - \cos(2\pi (f_\mathrm{s}/4) t)) & t < 1/(4f_\mathrm{s}) \\ \sin(2\pi f_\mathrm{s} t) & t > 1/(4f_\mathrm{s})\,. \end{cases}$$

Thereby, we obtain already after the first revolution of the point source a steady state solution at the monitoring point. That's why the result in Fig. 2 is displayed from 0.03s to 0.06s, which corresponds to the second revolution of the point source. The maximum amplitude error is computed by

$$F_\mathrm{amp} = \left| \frac{\psi_\mathrm{a,pp}^\mathrm{analytic}) - \psi_\mathrm{a,pp}^\mathrm{FEM}}{\psi_\mathrm{a,pp}^\mathrm{analytic}} \right| 100\,\%\,, \qquad (23)$$

where pp denotes the peak-peak-value within one revolution, and results in 0.21 %. In addition, we compute the

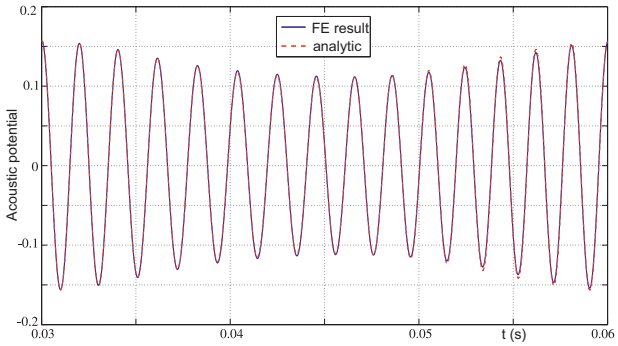

Figure 2: Acoustic potential at observation point.

phase error by summing up the absolute phase difference in each zero crossing between analytic and FEM solution within one revolution of the point source

$$F_\mathrm{phase} = \sum_{i=1}^{30} \left| \frac{\varphi_{i,\mathrm{zero}}^\mathrm{analytic} - \varphi_{i,\mathrm{zero}}^\mathrm{FEM}}{\varphi_{i,\mathrm{zero}}^\mathrm{analytic}} \right| 100\,\% \qquad (24)$$

Thereby, the phase error takes a value of 0.17 %.

Figure 2 displays the change of frequency over one revolution, which occures due to the Doppler effect. The acoustic signal at the receiver point changes its frequency f_o according to the position of the point source. Thereby, the instantaneous frequency f_inst is expressed by

$$f_\mathrm{inst} = \frac{f_\mathrm{s}}{1 - M_\mathrm{e} \cos\vartheta_\mathrm{e}}\,. \qquad (25)$$

In general, f_inst is defined by the time derivative of the signal's unwrapped phase

$$f_\mathrm{inst} = \frac{1}{2\pi} \frac{\partial \phi_\mathrm{o}}{\partial t}\,.$$

Numerically, we perform this operation by a phase demodulation using the *Matlab* functions unwrap and demod (see, e.g., [7]). Due to the numerical operations on the computed observation signal, we performed some filtering using a finite impulse response (FIR) filter to reduce numerical noise. The comparison between analytical and FE-based f_inst is displayed in Fig. 3.

Finally, we display the analytically computed acoustic pressure p_a according to (14) and the FE result obtained at the observation point in Fig. 4. Again one can see

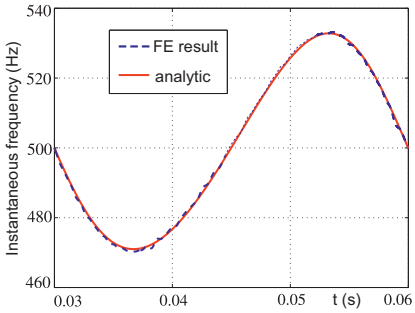

Figure 3: Comparison of instantaneous frequency.

the good agreement, which allows the conclusion that

our presented approach is well suited to perform numerical computations of acoustic fields including rotating domains. The computed relative amplite error according to

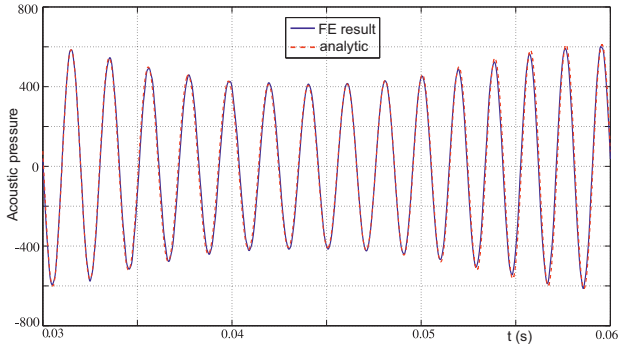

Figure 4: Acoustic pressure at observation point.

(23) results in 0.833 % and the phase error according to (24) to 2.5 %. The incresase in the phase error is mainly attributed to the time derivative and can be controlled by reducing the time step size or even better by a higher order time discretization scheme.

References

[1] P. Dowling, J. E. Ffowcs Williams: Sound and Sources of Sound. *Ellis Horwood Publishers, Chichester*, 1983

[2] J. Donea, A. Huerta, J. Ph. Ponthot, and A. Rodriguez-Ferran, *Encyclopedia of computational mechanics*, ch. Arbitrary Lagrangian-Eulerian methods, Wiley, 2004.

[3] M. Kaltenbacher: Numerical Simulation of Mechatronic Sensors and Actuators: Finite Elements for Multiphysics. Springer, 3rd ed., 2015.

[4] A. Hüppe, J. Grabinger, M. Kaltenbacher, A. Reppenhagen, G. Dutzler, W. Kühnel: A Non-Conforming Finite Element Method for Computational Aeroacoustics in Rotating Systems. *AIAA/CEAS Aeroacoustics Conference*, AIAA, 2014.

[5] T.J.R. Hughes: The Finite Element Method *Dover* 2000

[6] Kaltenbacher, B., Kaltenbacher, M., and Sim, I., A modified and stable version of a perfectly matched layer technique for the 3-d second order wave equation in time domain with an application to aeroacoustics, *Journal of Computational Physics*, 2013

[7] A. V. Oppenheim, R. W. Schafer, J. R. Buck: Discrete-Time Signal Processing. *Prentice-Hall*, 2nd ed., 1999.